DOI: 10.21062/mft.2025.050 © 2025 Manufacturing Technology. All rights reserved. http://www.journalmt.com

Overcoming Rotary Mechanism Limitations in CNC Machines: A 3-PRS Approach

Rudolf Madaj (0000-0003-2458-2351), Matúš Vereš (0009-0005-9469-3016), Róbert Kohár (0000-0001-7872-2829), Peter Weis (0000-0002-1669-4890), Filip Šulek

Faculty of Mechanical Engineering, University of Žilina in Žilina. Univerzitná 8215/1, 010 26 Žilina. Slovak Republic.

This paper presents the design and analysis of a 3-PRS mechanism for positioning cutting heads in CNC machines, addressing limitations of traditional rotary mechanisms such as hose twisting, wear, and limited modularity. Kinematic and dynamic analyses guided actuator selection and confirmed bearing durability. The mechanism achieves a favourable load-to-weight ratio and integrated Z-axis movement, making it suitable for simpler gantry CNC machines. Though programming is complex due to multi-axis synchronization, the modular design supports easy adaptation to different tools. Future research will focus on reducing the eccentric torch offset and refining dimensions to enhance versatility. The mechanism has strong potential in sectors like automotive, aerospace, and construction.

Keywords: Dynamic analysis, Engineering design, Kinematic analysis, Modular design, 3-PRS mechanism

1 Introduction

CNC cutting machines are automated devices designed for precise cutting and shaping of various materials. Their high accuracy and repeatability enable efficient mass production, ensuring that each component meets strict quality standards. Precise positioning of cutting heads is crucial for achieving desired cut quality, minimizing waste, and enhancing production efficiency [1-3].

Current positioning mechanisms have both advantages and disadvantages. While CNC machines achieve high precision and repeatability, their control and calibration can be complex, resulting in increased setup time and cost. Although flexibility and modularity are essential, many current mechanisms lack easy interchangeability of cutting heads, limiting their applicability. The positioning mechanisms include tilting and rotating heads, enabling desired cutting angles and enhancing CNC machine versatility. Several issues with existing rotary mechanisms must be resolved to enhance cutting performance [4–8].

Recent developments in reconfigurable CNC heads and modular end-effectors demonstrate the growing demand for lightweight, adaptable systems capable of rapid tool change and integration into hybrid kinematic structures [9-12]. This trend supports the shift toward mechanisms like 3-PRS for specialised applications. Traditional rotary mechanisms are complex due to numerous moving parts. This increases the risk of mechanical failures and makes troubleshooting more difficult. Cable management is challenging, as cable and hose twisting during rotation can lead to damage and disrupt operation. Limited range

of motion restricts the ability to achieve desired cutting angles and handle complex cuts efficiently. Current designs may lack rigidity, affecting cutting quality due to vibrations and instability [5, 13, 14].

Such twisting can shorten the lifespan of cables and hoses, further increasing maintenance costs. Special rotary hose couplings add complexity and cost. Limited modularity restricts their application across different tools and cutting head configurations. Rotation around multiple axes can accumulate errors, affecting overall accuracy. Complex calibration and control of individual axes increase setup demands and slow down production, especially for complex cutting tasks [15-17].

Recent research in multi-DOF CNC tool heads highlights the importance of modularity, compactness, and dynamic precision in complex cutting operations [8, 9, 14, 18]. In this context, 3-PRS architectures show potential for replacing traditional rotary heads in plasma and laser cutting machines [19-21].

This work proposes an efficient, modular mechanism to overcome the limitations of current rotary systems for positioning cutting heads. This new mechanism aims for high accuracy and repeatability while minimizing twisting and wear of transmission elements. It should be modular and easily adaptable to different cutting heads and applications, allowing easy assembly and disassembly to reduce maintenance costs and improve flexibility. Reducing the mechanism's weight and improving its dynamic performance will achieve higher speed and efficiency in cutting operations. The new mechanism should be applicable across various industrial sectors, including automotive, aerospace, and construction.

2 Methodology

2.1 Requirements of the Rotator

The new solution must meet several criteria: a torch tilt angle of at least 50°, a positioning speed matching the current rotator (130°.s-1), prevention of hose twisting and bending, and a minimum load capacity of 100 kg. The mechanism should be modular, enabling torch interchangeability and future scalability.

2.2 Selection of Mechanism

For this application, a spatial mechanism is required, making the 3-PRR mechanism unsuitable. Delta robots, while an option, have insufficient load capacity. Although the 3-RPR and 3-PRS mechanisms are similar, the latter is more commonly used in practice and was therefore selected. Additionally, a mechanism with more than three degrees of freedom (DOF) was not necessary for this application. Combined with X and Y movements of the CNC machine, the 3-PRS mechanism provides all the necessary motions and tilts for this application. Therefore, mechanisms with more DOF would be unnecessarily complex [22-35].

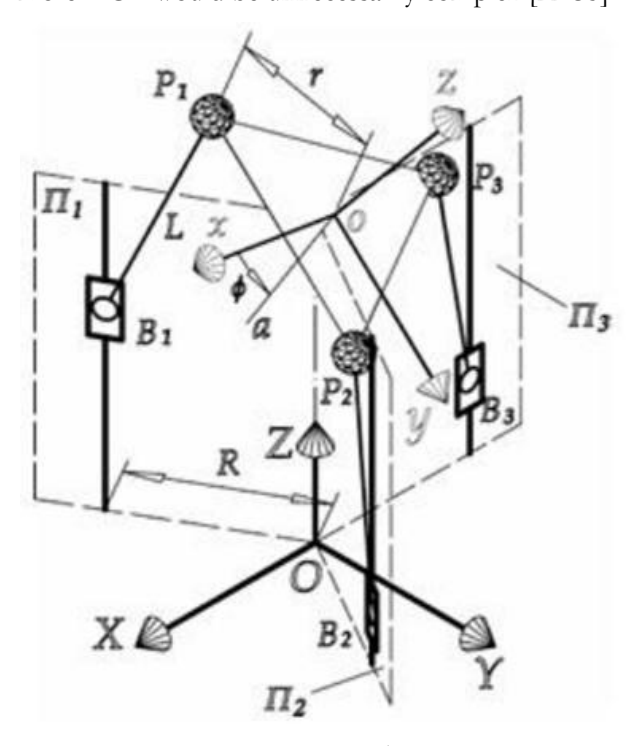


Fig. 1 Kinematic diagram

Figure 1 shows the kinematic diagram of the mechanism, consisting of two coordinate systems. The "O" system is the reference coordinate system, located at the center of the mechanism's fixed base. The second coordinate system, "o," is located at the center of the movable plate, where the plasma torch will be mounted. The mechanism includes three beams along which platforms (prismatic joints) move. Each platform is linked to the movable plate via a connecting arm.

A rotational joint is situated between the platform and the arm, while a spherical joint is located between the arm and the movable plate. The mechanism is designed to achieve a stroke length (Z-axis) of 400 mm. The dimension 'R' (the distance from the mechanism's center to the beam) was initially set to 200 mm. The diameter 'r' of the movable plate (i.e., the torch mount) was set to 115 mm, based on the largest torch size. The arm length "L" was selected to be 300 mm.

2.3 Design and Construction of the Mechanism

Several design variants of the key components were proposed. The base of the mechanism consists of a fixed and a movable platform (Figure 2a). This platform moves only along the Z-axis. t includes a fixed frame that contains an actuator integrated with a gearbox and pinion. The fixed frame also includes four linear guides (carriages). The movable platform, which includes a rack and linear guides, forms the second main part. The arm connects to the underside of the movable platform.

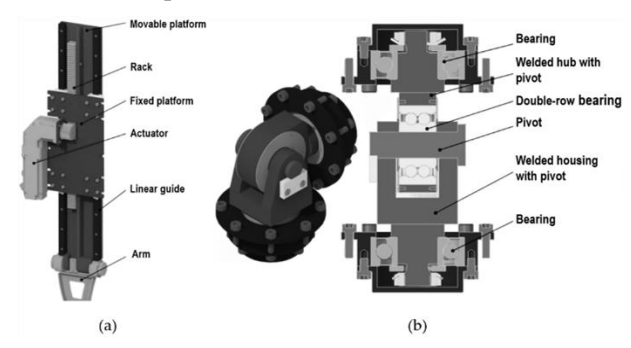


Fig. 2 Schematic of the moving platform (a); Cylindrical joint (b)

The arm (Figure 3a) is welded into an 'H'-shaped cross-section to maximise stiffness while minimising weight. The connection between the arm and the movable platform is secured by a simple pin, housed in two rolling bearings – tapered roller bearings 32002. A detail of the cylindrical joint is shown in Figure 2b.

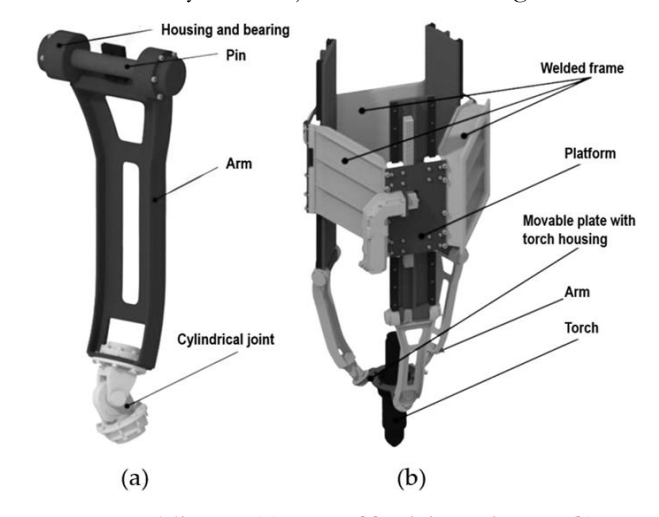


Fig. 3 The arm (a); Assembly of the mechanism (b)

2.4 Kinematic Analysis

Kinematic analysis was carried out to determine the required speeds and accelerations for each axis. This was necessary to size the actuators properly and to confirm the mechanism could perform the required motions. Kinematic and dynamic simulations were conducted using the PTC Creo Mechanism module (version 10.0) [36].

2.4.1 Critical Position Check

An extreme position analysis was performed to determine the mechanism's maximum tilt angles. Three positions were examined. In the first position, the torch is tilted directly under one arm. In the second position, the torch is tilted between two arms, on the opposite side compared to the first configuration. In the third position, the torch is tilted between the individual legs; it is not tilted directly under one arm as in the previous cases.

2.4.2 Horizontal Plane Analysis

Subsequently, kinematic analyses were performed in two planes - vertical and horizontal (XY). In the horizontal plane, two analyses were performed. The first analysis examined the torch's movement along the maximum trajectory (the perimeter of the working area). Only movement along the Z-axis was considered, as the X and Y axes were stationary during this analysis. The torch's movement in the XY plane was controlled solely by the mechanism (movement of all three platforms). The torch — specifically its cutting tip — had to maintain a constant height (i.e., no Zaxis movement). The torch was tilted to the required 50°. The analysis covered acceleration, one full rotation along the maximum trajectory, and subsequent deceleration. The torch's rotation speed was set at 130°.s-1 (as required). The tool's trajectory is shown in Figure 4. The results yielded the maximum speed and acceleration required for the platform drive. Additionally, the platform travel distance was measured to ensure that the stroke length was sufficient.

The second analysis in the horizontal plane involved rotating the torch about a fixed point. As in the previous analysis, the torch was tilted at an angle of 50°. In this case, the motion was achieved not only through the mechanism but also by moving the machine in the X and Y directions. The speeds and accelerations of the movable platforms were monitored again, with the maximum values remaining the same as in the previous test. Additionally, the speeds and accelerations in the X and Y directions were recorded. The displacements in the X and Y directions were also recorded, indicating how far the CNC machine must move to complete the rotation about a fixed point. Figure 5 shows the trajectories of all the movable platforms during the rotation around a single point.

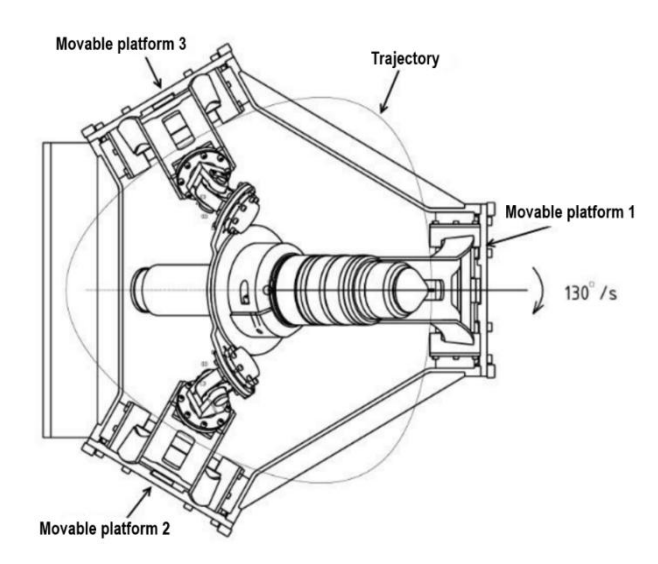


Fig. 4 First analysis trajectory (workspace perimeter)

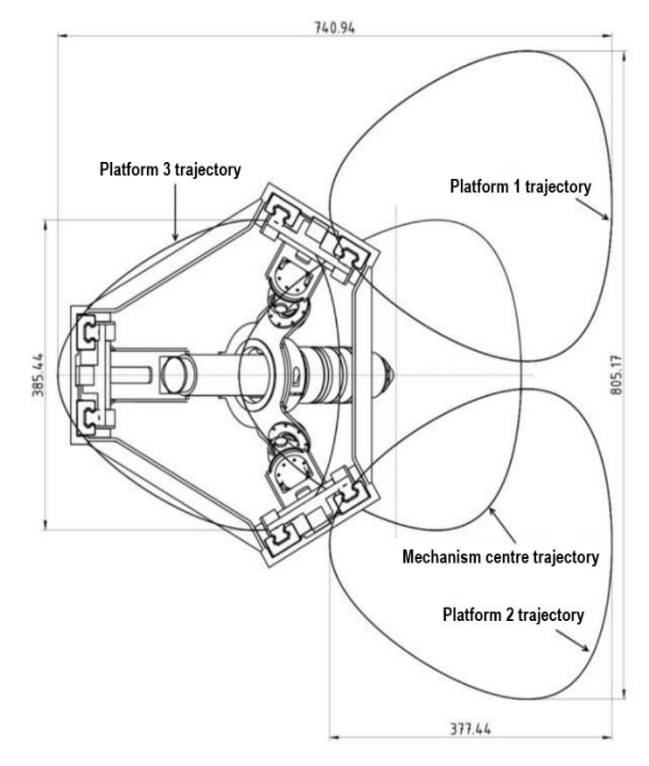


Fig. 5 Trajectories for rotations around a single point

2.4.3 Vertical Plane Analysis

The final kinematic analysis examined the movement in the vertical plane. The torch's movement was tracked from its outermost position (at a 50° tilt) to the centre of the mechanism and then returned to its starting position. The mechanism can be divided into three equal 120° sections. Due to their symmetry, analyses were limited to a representative 60° sector. The sector was subdivided into six planes, spaced 10° apart. Measurements were taken in all planes. The division of the mechanism into planes is shown in Figure 6. During the measurements, the speeds, accelerations, and displacements of the individual platforms were monitored.

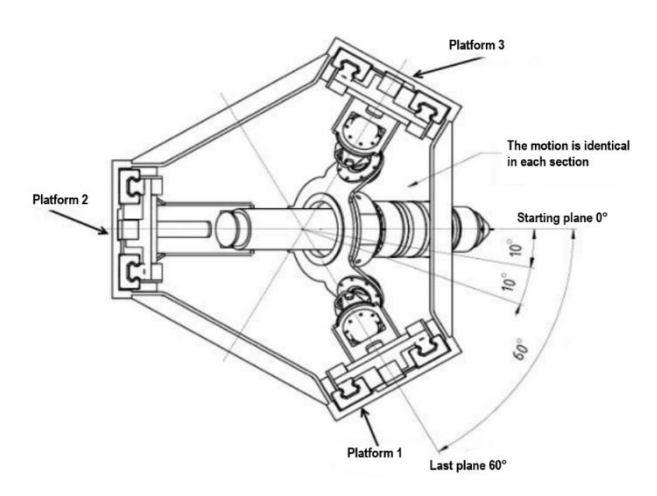


Fig. 6 Setting the analysis in the vertical plane

2.5 Dynamic Analysis

A dynamic analysis was carried out to evaluate the loads on various components during movement. The analysis measured axial and radial forces acting on the bearings at the arm joint (i.e., the connection between the arm and the movable platform). Forces on the pin in the cylindrical joint (or on the bearing housing the pin) and on the two angular contact bearings were also evaluated. Figure 7 illustrates the bearings that were monitored. Dynamic analysis was also conducted using PTC Creo Mechanism [36].

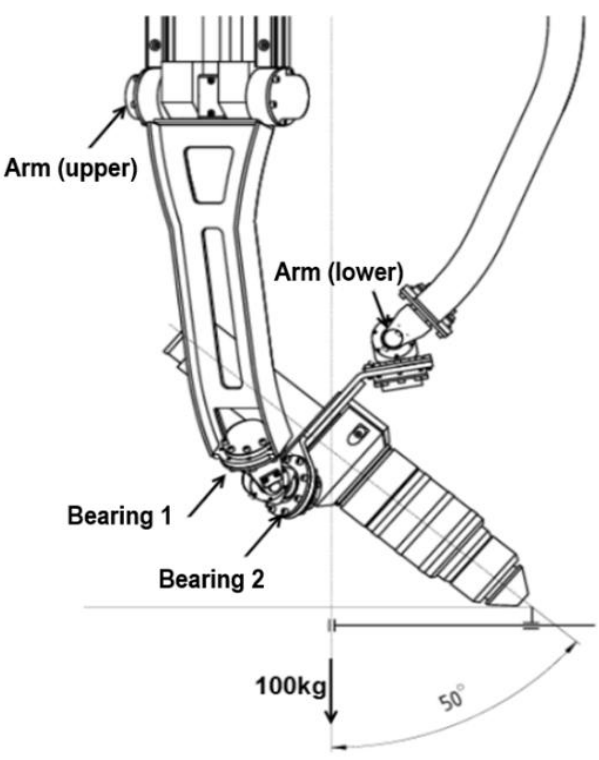


Fig. 7 Bearings monitored in dynamic analysis

The same speed and trajectory as in the kinematic analysis were used (i.e., movement along the working area perimeter), to evaluate the mechanism under maximum speed and acceleration conditions. Additionally, the movable plate (torch mount) was loaded

with a weight of 100 kg, in accordance with the initial requirements. This load was selected to ensure the mechanism's adaptability for future use with heavier equipment, such as a milling spindle.

3 Results and Discussion

3.1 Kinematic Analysis Outcomes

3.1.1 Critical Position Checks

The maximum tilt angle in the first position is 72° (shown in Figure 8a), while the maximum tilt angle in the second position is 103° (Figure 8b).

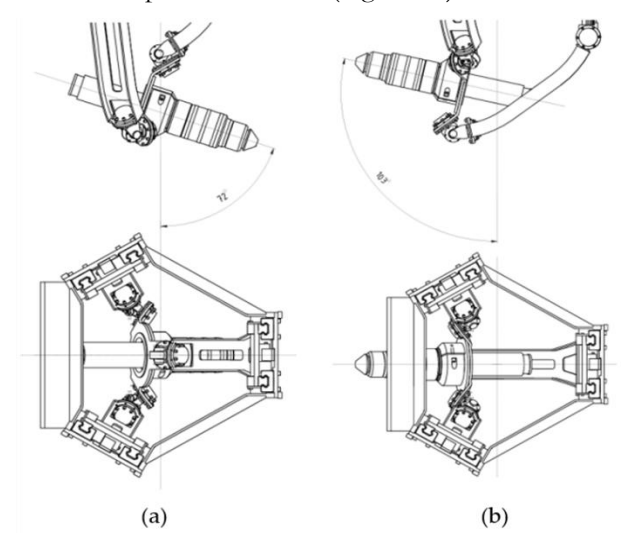


Fig. 8 Critical position 1 (a); Critical position 2 (b)

The maximum tilt angle in the third position is 83° (Figure 9a). However, in this position, an undesirable effect occurs – the torch is eccentrically displaced from the center of the mechanism. The displacement from the center is 48 mm. The second position is also the most critical in terms of potential hose and arm collisions, thus the maximum tilt angle is limited to 55° (shown in Figure 9b).

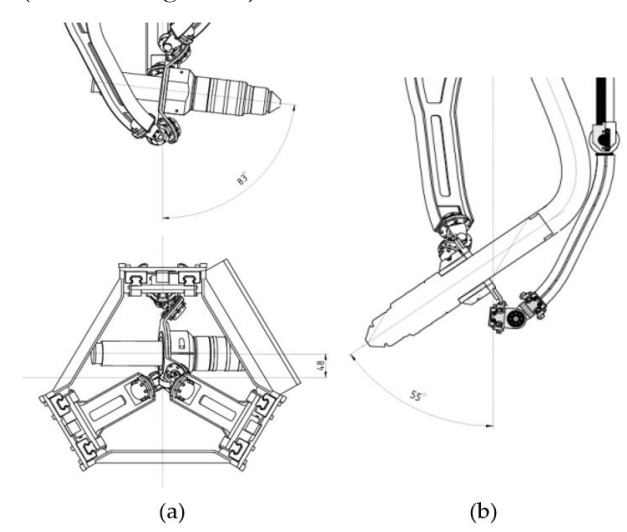


Fig. 9 Critical position 3 (a); Critical position 2 with hose (b)

3.1.2 Maximum Trajectory

The measurement results for movement along the maximum trajectory are shown in Figure 10. The graphs indicate that the total distance traveled by the platforms was 170.9 mm. The maximum speed reached by one of the platforms was 0.87 m.s⁻¹. The highest acceleration achieved was 14.34 m.s⁻².

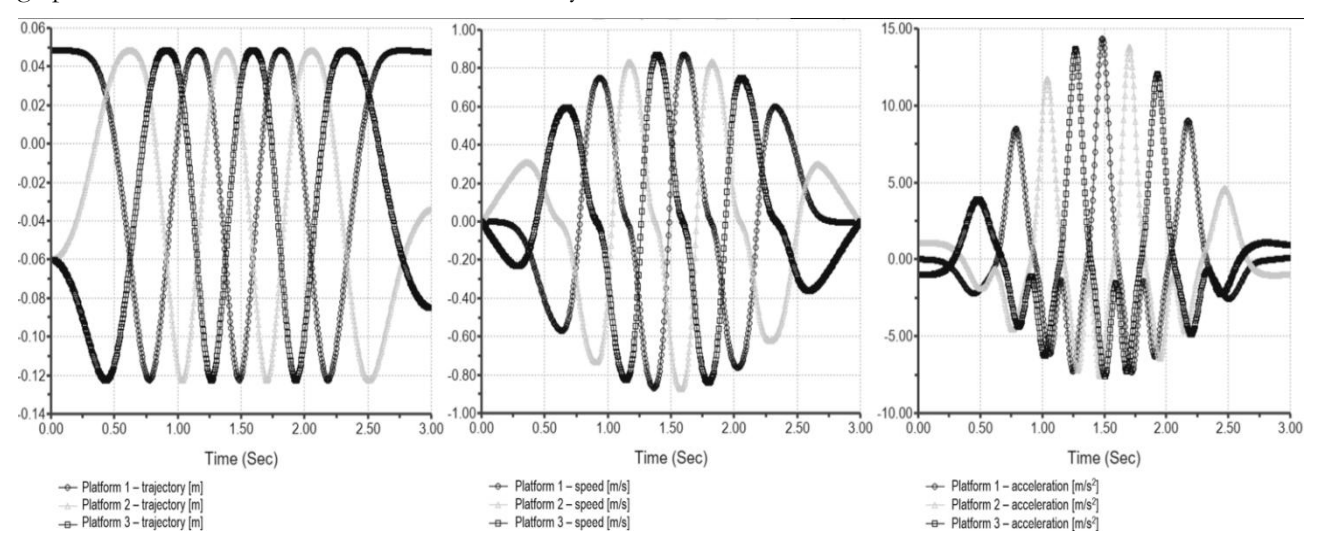


Fig. 10 Plots of platform trajectories (left), velocities (middle), accelerations (right)

3.1.3 Rotation Around a Point

During rotation about a single point, platform speeds and accelerations were measured, as shown in

Figure 11. The maximum values for speed and acceleration were the same as in the previous measurement.

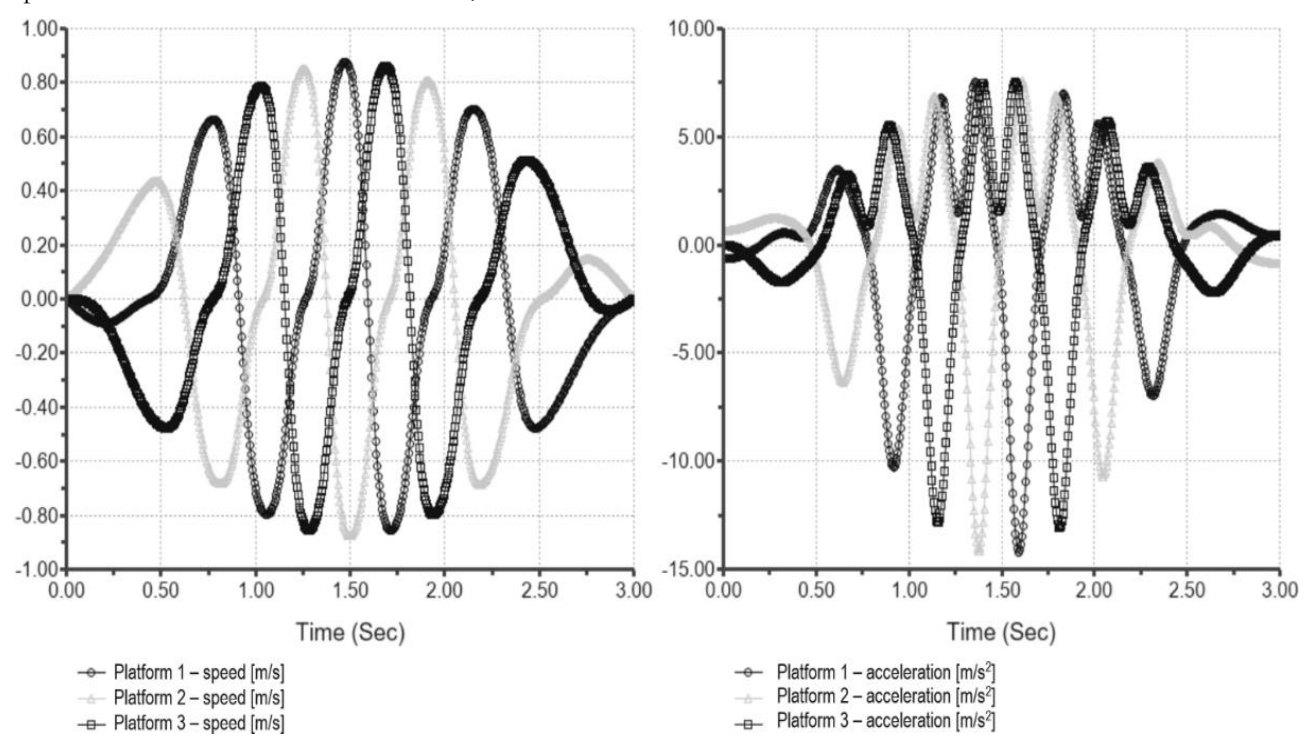


Fig. 11 Plot of velocities (left) and accelerations (right) for rotation around a point

The speeds and accelerations in the X and Y axes were also monitored. The results of these measurements are shown in Figures 12 and 13. The maximum speed in the X direction was 2.25 m.s⁻¹, and in the Y direction, it was 2 m.s⁻¹. The maximum acceleration for both directions was 22.5 m.s⁻². However, motion along these axes is executed by the CNC

machine, not the mechanism itself. To ensure the required positioning speed, the CNC machine's drives must support these velocity and acceleration values.

The displacements required in the X and Y axes were also measured (Figure 14). The machine moved 400 mm in the X direction and 385 mm in the Y direction.

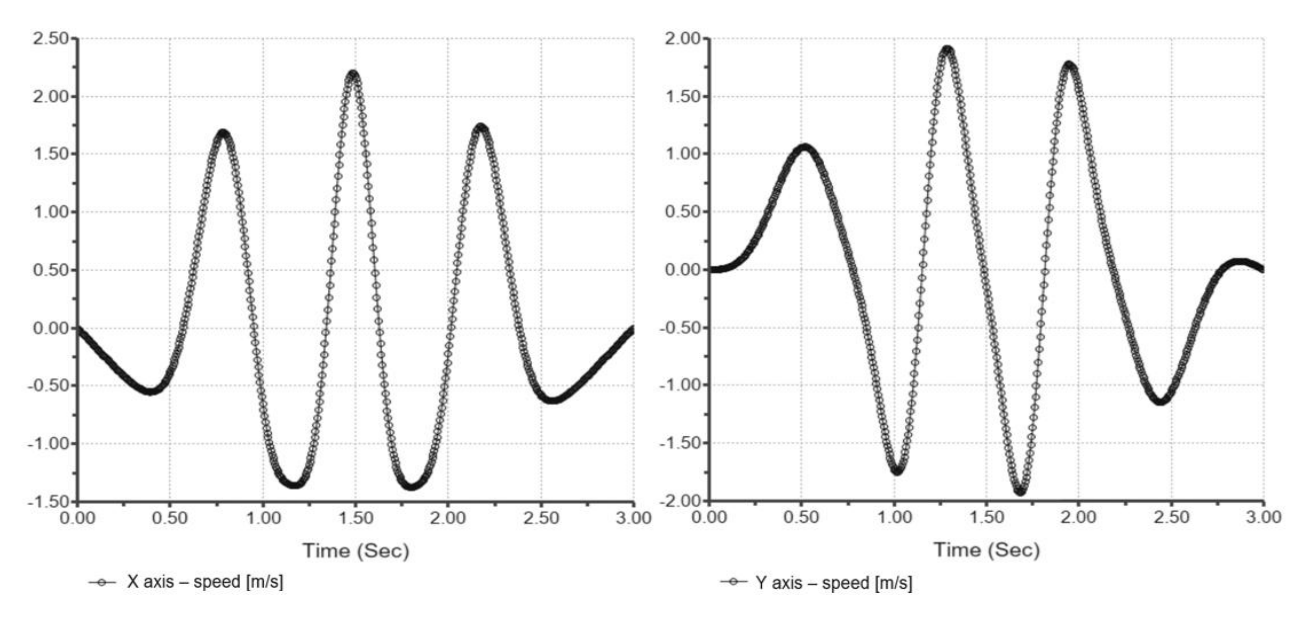


Fig. 12 Plots of velocities for X and Y axes

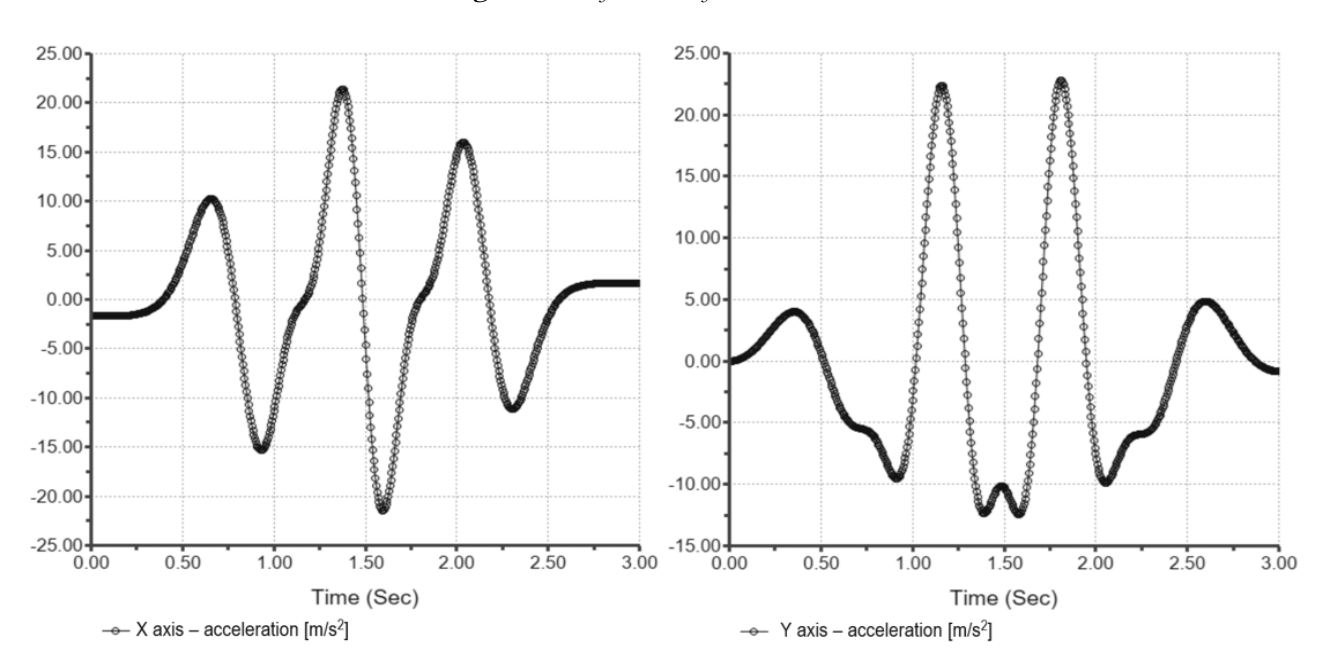


Fig. 13 Plots of accelerations for X and Y axes

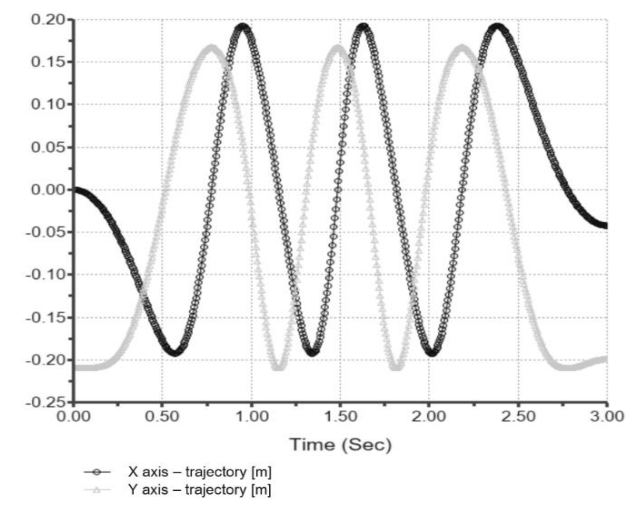


Fig. 14 Plot of X and Y axis trajectories

3.1.4 Vertical Plane

In the vertical plane, a total of six measurements were conducted n six angular sections. Due to the scope of the article, graphs of speeds, accelerations, and trajectories will be presented only for the case with the highest recorded values (shown in Figure 15). These values were measured in the 60° plane. During this operation, two platforms followed identical trajectories, resulting in the same measured values. A sudden change in acceleration was observed, attributed to the design of the spherical joint. The maximum values of speeds and accelerations resulting from this analysis are lower than those recorded during the maximum trajectory. The platforms' total travel distance was the same as in the horizontal plane test.

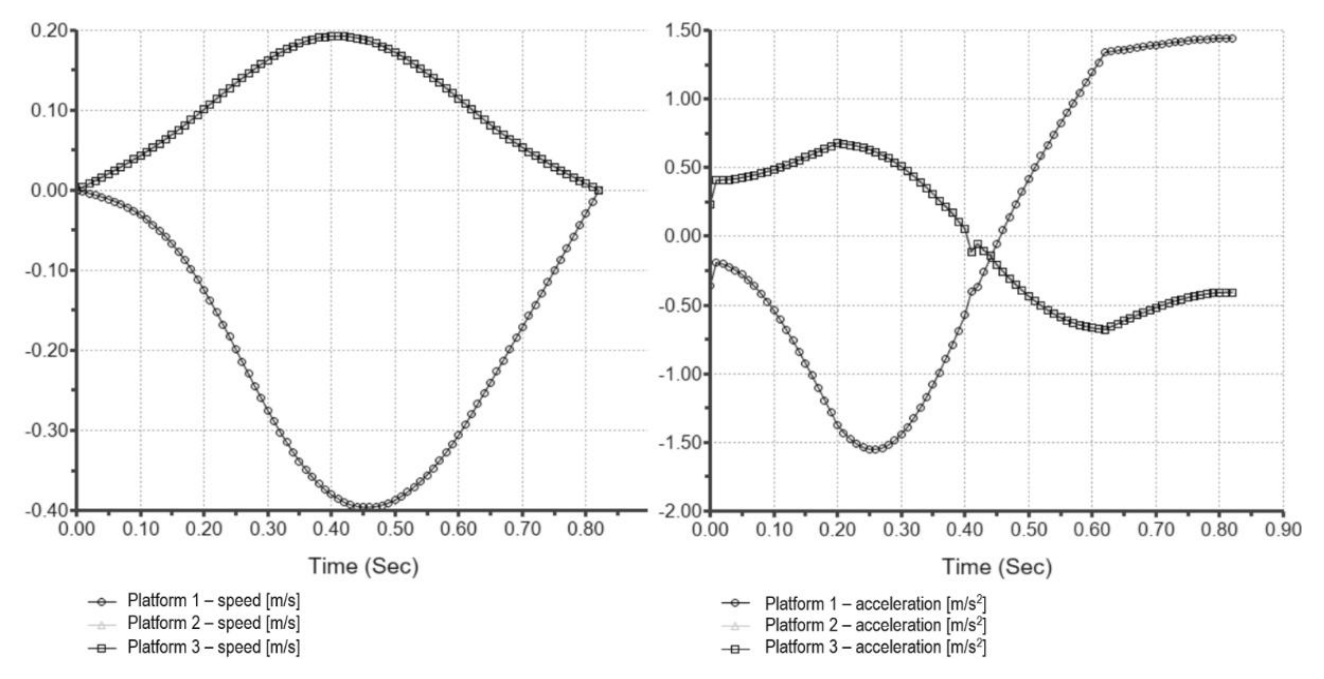


Fig. 15 Plots of velocities (left) and accelerations (right) for 60° plane

3.2 Dynamic Analysis Findings

The dynamic analysis resulted in graphs (Figures 16 and 17) that show the axial and radial forces acting on the bearings.

The resultant force acting on the bearing was calculated using the Pythagorean theorem:

$$F_c = \sqrt{F_{a_{max}}^2 + F_{r_{max}}^2} \tag{1}$$

Where:

F_c...The resultant force;

F_a...The axial force;

F_r...The radial force.

Resulting values are recorded in Table 1.

Tab. 1 Forces acting on individual bearings

| Part | Axial Force [N] | Radial Force [N] | Resultant Force [N] |
|-------------|-----------------|------------------|---------------------|
| Arm (upper) | 757 | 295 | 812.5 |
| Arm (lower) | 532 | 717 | 892.8 |
| Bearing 1 | 532 | 773 | 938.4 |
| Bearing 2 | 434 | 650 | 781.6 |

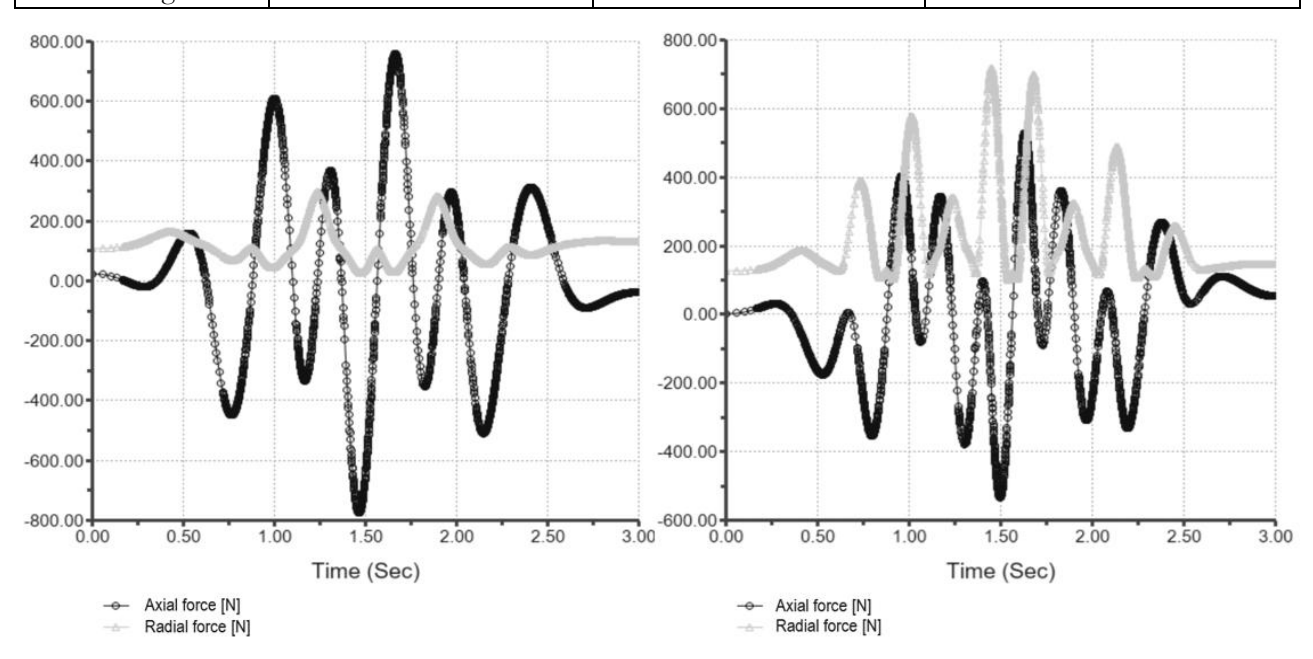


Fig. 16 Plot of axial and radial forces acting on the measured connections: upper arm bearing (left) and lower arm bearing (right)

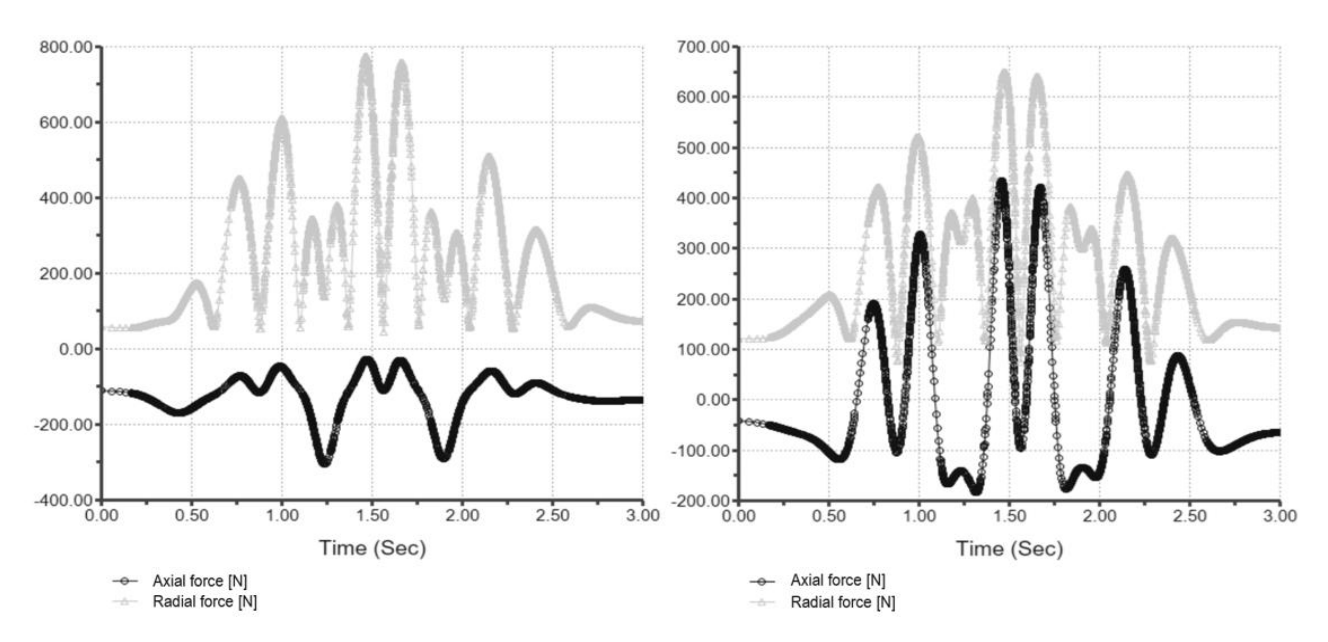


Fig. 17 Plot of axial and radial forces acting on the measured connections: bearing 1 (left), bearing 2 (right)

A static and dynamic check was performed for all bearings based on the bearing manufacturer's recommendations [37] to verify if the selected bearings could withstand the applied loads. The check confirmed that all bearings meet the required load conditions. Since the load calculation included the mechanism's load capacity of 100 kg in addition to its own weight, the resultant bearing lifespan will be higher because the plasma torch used in this application is relatively light. Nevertheless, the calculation indicated that even at maximum machine load, no deformations should occur in the bearings.

3.3 Performance Evaluation

A key benefit of the proposed mechanism is that it prevents twisting and bending of the torch hose. The hose conflicts with the arm in position 2, as shown in Figure 9. However, this conflict occurs at a tilt of 55°, which is greater than the required tilt angle. In other positions, the mechanism can tilt even more. This additional range can be used when higher tilt angles are needed. Limiting torch tilt in the critical position during programming allows greater tilt angles to be used elsewhere. This enhances the versatility of the machine.

The mechanism achieves a favourable load-to-weight ratio, outperforming Delta mechanisms and the original rotator, both of which had significantly lower load capacities and significantly greater weight. Another key advantage is the integrated Z-axis motion, enabling the tool to be positioned vertically without relying on the CNC machine. The original rotator, like many other mechanisms, lacks this feature, requiring the CNC machine to perform movements in all three axes. As a result, the new mechanism can be installed on simpler gantry-type CNC machines with only two axes of motion.

The new mechanism is modular, allowing the movable plate to be replaced with one that accommodates different torch types or other tools. An improvement would be to redesign the movable plate so that only the clamping element needs replacement, not the entire plate.

The required positioning speeds were achieved, and the drives were dimensioned accordingly through kinematic analysis. It is possible to select drives capable of achieving higher acceleration values, thereby reaching positioning speeds higher than originally required. However, increasing speeds would require re-evaluating the bearing durability.

The mechanism's performance is limited by the CNC machine's X and Y drive capabilities. To achieve the desired positioning speed, the requirements for speed and acceleration in these directions must be met. However, not all CNC machines meet these parameters, so the actual positioning speed may be lower in practice.

One drawback is the mechanism's complexity, which makes motion programming more difficult. It is necessary to synchronize the movements of all three platforms and coordinate them with the drives of the X and Y axes. In this regard, traditional rotators are a simpler choice.

In certain positions, the torch is undesirably offset from the center of the mechanism. This increases the complexity of an already complicated motion programming process. This offset also results in a triangular rather than circular working area.

Further development should aim to eliminate or reduce the torch offset. Optimizing the mechanism's dimensions could help reduce both the torch offset and the demands on the X and Y drives. This step would enhance the versatility of the proposed solution.

4 Conclusion

This research proposed and validated a novel 3-PRS mechanism designed to overcome key limitations of traditional rotary systems in CNC machines, such as hose twisting, limited modularity, and high wear rates. Comprehensive kinematic and dynamic analyses confirmed that the mechanism met all key performance requirements, including 130°.s⁻¹ positioning speed, 100 kg load capacity, and a tilt angle exceeding the target. Crucially, the integrated Z-axis movement enhances versatility, enabling simpler two-axis gantry machines to perform complex positioning tasks.

Despite these benefits, some challenges remain—particularly the complexity of motion programming due to required multi-axis synchronization, and an eccentric torch offset in certain positions. This offset limits the effective working area. Future work will aim to overcome these limitations by minimizing eccentric offsets through design optimization and simplifying control algorithms. With further improvements in scalability and adaptability, the mechanism shows strong potential for widespread industrial use, enhancing the efficiency and reliability of CNC machining.

Acknowledgement

The authors acknowledge the financial support from the project 1/0568/24: Research in the Area of Load and Stress-Strain States of Bearing Cages, which made this research possible.

References

- [1] SAKTI, S. P., NURWARSITO, H., SUPRAYOGO, D., PRAYOGO, C., & KUSUMA, A. S. (2021). Automation of CNC Machinery in Improving Quality and Production Speed of Agricultural Product Processing Machinery Components. 6th In 2021 IEEE International Conference on Recent Advances and Innovations in Engineering (ICRAIE), pp.1-5, doi:10.1109/ICRAIE52900.2021.9704031
- [2] ZHANG, J. (2018). Research on CNC Lathe Programming and Improving Machining Accuracy. *IOP Conf. Ser.: Mater. Sci. Eng.* 452 042050, doi: 10.1088/1757-899X/452/4/042050
- [3] GHERGHEA, I. C., BUNGAU, C. & NEGRAU, D. C. (2019). Lead time reduction and increasing productivity by implementing lean manufacturing methods in cnc processing center. *IOP Conf. Ser.: Mater. Sci. Eng.* 568 012014, doi: 10.1088/1757-899X/568/1/012014

- [4] ZHAO, X. M., YANG, G. Y., & SHAO, H. (2004). The Influence of Cutting Edge Orientation and Spindle Motion Error on Machined Surface in Milling. In: *Key Engineering Materials* (Vols. 259–260, pp. 415–420). Trans Tech Publications, Ltd. https://doi.org/10.4028/www.scientific.net/kem.259-260.415
- [5] WEN, J., XIE, F., LIU, X., & YUE, Y. (2023). Evolution and Development Trend Prospect of Metal Milling Equipment. *Chin. J. Mech. Eng.* 36, 33 (2023). https://doi.org/10.1186/s10033-023-00865-x
- [6] ZAWADA-MICHAŁOWSKA, M., PIEŚKO, P., & LEGUTKO, S. (2023). Effect of the cutting tool on the quality of a machined composite part. *Manufacturing Technology 2023*, 23(6):870-879. DOI: 10.21062/mft.2023.107
- [7] PADAYACHEE, J., & BRIGHT, G., (2012). Modular machine tools: Design and barriers to industrial implementation. *Journal of Manufacturing Systems*, 31, pp. 92-102. https://doi.org/10.1016/j.jmsy.2011.10.003
- [8] QUISPE, M., CASTILLO, C., CASTRO, J., & PONCE, A. (2023). Design and Implementation of a Pick and Place System Using a 4 DOF Robotic Arm Integrated into a Longitudinal Horizontal Movement Base. LACCEI, 1(8). https://doi.org/10.18687/LACCEI2023.1.1.794
- [9] KRIMPENIS, A. A., & IORDANIDIS, D. M. (2023). Design and analysis of a desktop multiaxis hybrid milling-filament extrusion CNC machine tool for non-metallic materials. *Machines*, 11(6), 637. https://doi.org/10.3390/machines11060637
- [10] WANG, D., WU, J., WANG, L. & LIU, Y. A Postprocessing Strategy of a 3-DOF Parallel Tool Head Based on Velocity Control and Coarse Interpolation. *IEEE Transactions on Industrial Electronics*, vol. 65, no. 8, pp. 6333-6342, Aug. 2018, doi: 10.1109/TIE.2017.2784378.
- [11] XIE, F., LIU, X. J., & WANG, J. (2012). A 3-DOF parallel manufacturing module and its kinematic optimization. *Robotics and Computer-Integrated Manufacturing*, 28(3), 334-343. https://doi.org/10.1016/j.rcim.2011.10.003
- [12] BELORIT, M., HRCEK, S., GAJDOSIK, T., & STEININGER, J. (2017, September). Description of the bearing check program for countershaft gearboxes. In Proceeding of 58th International Conference of Machine Design Departmens (ICDM) (pp. 32-35).

- [13] YI, X., XU, T., MA, W., YAN, Z. & GAO, D. (2010). 5-axis CNC Whirlwind Milling Method on Helical Surfaces of PDM's Rotors, *Internati*onal Conference on Measuring Technology and Mechatronics Automation, Changsha, China, 2010, pp. 7-10, doi: 10.1109/ICMTMA.2010.498.
- [14] YINTAO, H., JINWEI, W., BAIMING, L., & RONGSHENG, C. (2024, November). Research on Processing Precision of Multi-Frequency Plasma CNC Machining Centers. In 2024 Cross Strait Radio Science and Wireless Technology Conference (CSRSWTC) (pp. 1-3). IEEE.

 10.1109/CSRSWTC64338.2024.10811520
- [15] CHU, A.M., LE, M. T., HOANG, N. H., et al. (2024). A framework for practically effective creation of postprocessors for 5-axis CNC machines with all possible configurations and working mechanisms. *Proceedings of the Institution of Mechanical Engineers, Part B: Journal of Engineering Manufacture.* 2024;238(5):682-694. doi:10.1177/09544054231179314
- [16] XIONG, Q., & ZHOU, Q. (2020). Development Trend of NC Machining Accuracy Control Technology for Aeronautical Structural Parts. World Journal of Engineering and Technology. Vol(8). 10.4236/wjet.2020.83022
- [17] BAOYU, S., & HONGTAO, W. (2020). Kinematics analysis of a new parallel robotics. *International Journal of Advanced Robotic Systems*, 17(2), 1729881420919950.
- [18] TUGEUMWOLACHOT, T., SEKI, H., TSUJI, T., & HIRAMITSU, T. (2022, August). Development of a multi-dof cutting tool with a foldable supporter for compact in-pipe robot. In 2022 IEEE International Conference on Mechatronics and Automation (ICMA) (pp. 587-592). IEEE. 10.1109/ICMA54519.2022.9856115
- [19] WU, H., KONG, L., LI, Q., WANG, H., & CHEN, G. (2023). A comparative study on kinematic calibration for a 3-DOF parallel manipulator using the complete-minimal, inverse-kinematic and geometric-constraint error models. *Chinese Journal of Mechanical Engineering*, 36(1), 121. https://doi.org/10.1186/s10033-023-00940-3
- [20] ELGAMMAL, A. T., MAGDY, M., & LASHIN, M. (2024). Learning complex nonlinear dynamics of a 3D translational parallel manipulator using neural network. *Heliyon*, 10(18). 10.1016/j.heliyon.2024.e37669
- [21] GHASEMI, J., MORADINEZHAD, R., & HOSSEINI, M. A. (2019). Kinematic synthesis

- of parallel manipulator via neural network approach. *arXiv* preprint arXiv: 1904.04668. https://doi.org/10.48550/arXiv.1904.04668
- [22] TLUSTY, J., ZIEGERT, J., & RIDGEWAY, S. (1999). Fundamental Comparison of the Use of Serial and Parallel Kinematics for Machines Tools. CIRP Annals. 48, pp. 351-356. https://doi.org/10.1016/S0007-8506(07)63200-4
- [23] CÉZOVÁ, E. (2025). Demonstration of Neural Network in Prediction of Bearing Lifetime. *Manufacturing Technology*, 25(2), 170-173. DOI: 10.21062/mft.2025.017
- [24] VISCHER, P., & CLAVEL, RE. (1998). Kinematic calibration of the parallel Delta robot. *Robotica*. 16. 207 218. 10.1017/S0263574798000538.
- [25] RUSSO, M., ZHANG, D., LIU, X., & XIE, Z. (2024). A review of parallel kinematic machine tools: Design, modeling, and applications. *International Journal of Machine Tools and Manufacture*. Vol. 196. https://doi.org/10.1016/j.ijmachtools.2024.104118
- [26] WU, X. (2019). Optimal Design and Singularity Analysis of a Spatial Parallel Manipulator. *Symmetry* 11, no. 4: 551. https://doi.org/10.3390/sym11040551
- [27] WANG, D., WU, J., WANG, L. & LIU, Y. A Postprocessing Strategy of a 3-DOF Parallel Tool Head Based on Velocity Control and Coarse Interpolation. *IEEE Transactions on Industrial Electronics*, vol. 65, no. 8, pp. 6333-6342, Aug. 2018, doi: 10.1109/TIE.2017.2784378.
- [28] DRÍMALOVÁ, P., NOVÝ, F., UHRIČÍK, M., VÁŇOVÁ, P., ŠIKYŇA, L., CHVALNÍKOVÁ, V., & SLEZÁK, M. (2024). Effect of change in current density on hydrogen embrittlement of advanced high-strength steel S960MC during hydrogenation. *Manufacturing Technology*, 24(1), 40-46. DOI: 10.21062/mft.2024.010
- [29] ENFERADI, J., TAVAKOLIAN, M. (2017). Lagrangian Dynamics Analysis of a XY-Theta Parallel Robotic Machine Tool. *Periodica Polytechnica Mechanical Engineering*. 61(2), pp. 107–114, 2017. https://doi.org/10.3311/PPme.9368
- [30] ČERNOHLÁVEK, V., KLIMENDA, F., SUSZYNSKI, M., ŠTĚRBA, J., & ZDRÁHAL, T. (2024). Optimizing Manufacturing Technology: Unraveling Symmetry in Cubic Equation Roots. *Manufacturing Technology*, 24(5), 731-737. DOI: 10.21062/mft.2024.077

- [31] HAJDUCIK, A., SKRABALA, J., MEDVECKY, S., & BRUMERCIK, F. (2019). Kinematic Analysis of Trapezoidal Suspension. Scientific Journal of Silesian University of Technology-Series Transport. Vol.(104). Pp. 27-36. doi: 10.20858/sjsutst.2019.104.3
- [32] ŠTEININGER, J., HRČEK, S., SMETANKA, L., & SKYBA, R. (2020). Optimisation procedure of inner geometry in spherical roller bearings with regard to their durability. Zeszyty Naukowe. *Transport/Politechnika Śląska*. DOI 10.20858/sjsutst.2020.106.15.
- [33] CHEN, X., LIU, X-J., XIE, F., SUN, T. (2014) A Comparison Study on Motion/Force Transmissibility of Two Typical 3-DOF Parallel Manipulators: The Sprint Z3 and A3 Tool Heads. *International Journal of Advanced Robotic* Systems. 2014;11(1). doi:10.5772/57458
- [34] BLATNICKÝ, M., DIŽO, J., MOLNÁR, D., & ISHCHUK, V. (2023, August). Structural

- Design of a Rotary Valve Manipulator of Bulk Materials–Strength Design of Connecting Elements of the Frame and Trolley. In *Manufacturing Technology 2024*, 24(6):871-878. DOI: 10.21062/mft.2024.096
- [35] YOUSSEF, F., & KASSNER, S. (2023). Kinematic Design. In: Kern, T.A., Hatzfeld, C., Abbasimoshaei, A. (eds) Engineering Haptic Devices. *Springer Series on Touch and Haptic Systems*. Springer, Cham. https://doi.org/10.1007/978-3-031-04536-3_8
- [36] PTC Inc. (2018). Ptc Creo Parametric TOOLKIT User's Guide. Retrieved from https://support.ptc.com/images/cs/articles/2018/05/1525425932uNM3/tkuse.pdf
- [37] SKF Group. (2019, 03). Valivá ložiska. *SKF*. https://cdn.skfmediahub.skf.com/api/public/0901d1968096351e/pdf_preview_medium/0901d1968096351e_pdf_preview_medium.pdf#cid-121486